Available online at www.sciencedirect.com
SCIENCE DIRECT®
Nuclear Instruments and Methods in Physics Research A 497 (2003) 429–439
NUCLEAR INSTRUMENTS & METHODS IN PHYSICS RESEARCH Section A
www.elsevier.com/locate/nima

SACI—a 4π plastic phoswich array ancillary detector system of a γ-ray spectrometer

J.A. Alcántara-Núñez[a,*], J.R.B. Oliveira[a], E.W. Cybulska[a], N.H. Medina[a], M.N. Rao[a], R.V. Ribas[a], M.A. Rizzutto[a], W.A. Seale[a], F. Falla-Sotelo[a], F.R. Espinoza-Quiñones[b], C. Tenreiro[c]

[a] *Depto. Fisica Nuclear, Instituto de Fisica, Universidade de São Paulo, Caixa Postal 66318, São Paulo, SP 05315-970, Brazil*
[b] *Dep. de Eng. Química, Universidade Estadual do Oeste do Paraná (UNIOESTE), Toledo, PR, Brazil*
[c] *Facultad de Ciencias, Universidad de Chile, Santiago de Chile, Chile*

Received 13 August 2002; received in revised form 11 October 2002; accepted 24 October 2002

Abstract

A large solid angle low-Z charged particle detector system was built in order to improve the quality of the identification and selection of evaporation channels for in-beam γ-spectroscopy measurements. The array consists of 11 plastic phoswich telescopes closely packed in a 4π arrangement and to be used as an ancillary system for the Pelletron Laboratory γ-ray spectrometer. The new system was tested in *γ-particle* and *γ–γ-particle* coincidence measurements using the ^{27}Al $+^{16}$ O and ^{100}Mo $+^{11}$ B reactions, at 53 and 43 MeV incident beam energies, respectively. The values for the particle detection efficiency and improvement in the peak to background ratios are considered acceptable for the usefulness of the system.

PACS: 29.30.-h; 29.30.Ep; 29.30.Kv; 29.40.Mc

Keywords: γ-ray spectroscopy; Ancillary detectors; Phoswich telescope detectors; Light-charged particles spectroscopy

1. Introduction

The γ-ray spectroscopy of low-Z or very neutron deficient evaporation residues is difficult because of the strong competition among many open channels. Typically 2–5 particles are evaporated from a heavy-ion reaction, in varied combinations of protons, neutrons and alpha particles. To overcome the problem of identification and the study of exotic or rare nuclei populated with low cross-sections, ancillary systems are often used as a filtering device for a γ-ray spectrometer. Some of these systems have the capability to identify reaction channels which involve the emission of light charged particles or neutrons; other systems can separate the residual channels by identifying the mass of the recoiling nuclei (Recoil Mass Spectrometer). In many cases these systems allow isolation of the signal of interest with a much

*Corresponding author. Tel.: +55-11-3091-6942; fax: +55-11-3031-2742.
E-mail address: juan.alcantara@dfn.if.usp.br (J.A. Alcántara-Núñez).

0168-9002/03/$ - see front matter
PII: S0168-9002(02)01926-5

higher efficiency than provided by detecting only the emitted γ-rays. In a specific case, a partial selection of one or more particular channels, made by detecting and identifying some or all of the evaporated charged particles obtained using ancillary charged particle detectors, could significantly enhance the *resolving power* (conventionally defined as the improvement factor of the peak to background ratio) of the system. This is reflected in the increase of the detection sensitivity. In this way, many laboratories in the world have used ancillary detectors in conjunction with γ-ray spectrometers. For example, at INFN, Legnaro, Italy, a system of 40 $\Delta E - E$ silicon surface barrier detectors *Italian Silicon Sphere* (ISIS) [1] is used together with the γ-ray spectrometer GASP. At LBNL, Berkeley, USA, a system of 96 $\Delta E - E$ CsI (Microball) [2] is used together with the Gamasphere. In this paper the construction and performance of a 4π charged particle spectrometer, *Sistema Ancilar de CIntiladores* (SACI), is reported. It was built to operate as a modular ancillary detector system in conjunction with the Pelletron Laboratory γ-ray spectrometer [3], named *Pequeno Espectrômetro de Radiação Electromagnética com Rejeição de Espalhamento* (PERERE) at the University of São Paulo, Brazil.

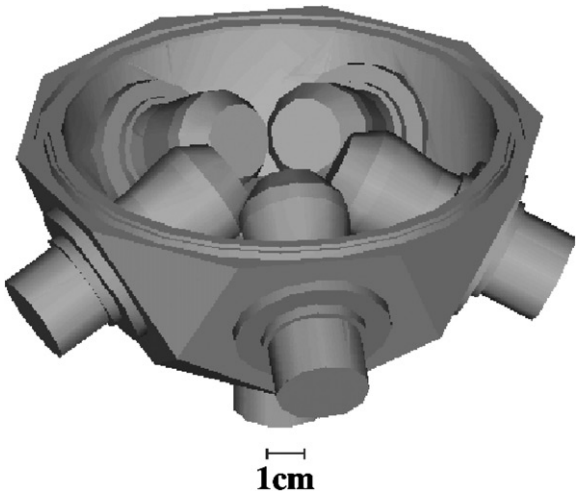

Fig. 1. View of the target chamber (SACI).

2. The SACI telescope multidetector setup

The new detector should have a few main requirements: First, it must discriminate between protons and alpha particles. Also, it must have high detection efficiency, and therefore should cover as much of the 4π solid angle as possible. Finally, it should have good resistance to radiation damage, transparency to γ-radiation and low cost.

The SACI device, consists of 11 plastic phoswich scintillators, arranged in the geometry of a dodecahedron. The design of the 4π charged particle telescope array was based on Ref. [4]. The target chamber is a hollow semi-regular polyhedron with 12 pentagonal and 20 triangular faces and serves as the support for the detectors (see Fig. 1). It is built of aluminium and is divided in two hemispheres with thin walls in order to minimize γ-ray absorption. The beam enters the vacuum chamber through a flange in one of the pentagonal faces. The chamber has a diameter of 14 cm, and the entire system, including the photomultiplier tubes and bases fits in a sphere of 24 cm diameter.

Each phoswich telescope consists of a 0.1 mm thick fast scintillation (BC400, decay time 2.4 ns) ΔE detector bonded to a 10 mm thick long decay time (BC444, decay time 264 ns) E detector, (both from BICRON [5]). The detector faces have a diameter of 2 cm. They cover 76% of the 4π solid angle. The E and ΔE detectors were bonded together by the vacuum heat press technique in order to avoid the presence of a dead layer [6,7]. In this way, the thin ΔE plastic scintillator was heat-pressed to the E scintillator block (see Fig. 2), inside a vacuum chamber in order to eliminate the possibility of trapping air bubbles between these two scintillators and to avoid the presence of light traps or a dead layer between them. The bonding was performed under a vacuum of the order of 10^{-3} Torr. A load of $\approx 400\ \mathrm{g/cm^2}$ was used to provide the pressure on the scintillators over a copper block at $\approx 76^{\circ}\mathrm{C}$. The choice of temperature is very critical because, at a higher temperature, there may be deterioration of the mechanical, optical and scintillating properties and, at a lower temperature bonding is not achieved. A full

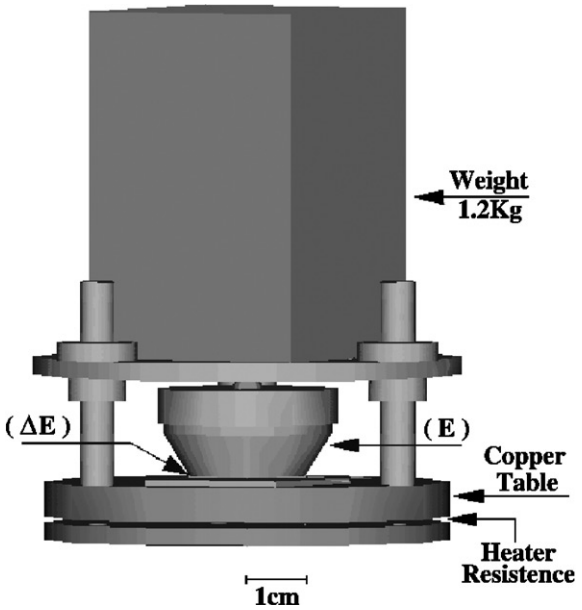

Fig. 2. Heat press setup.

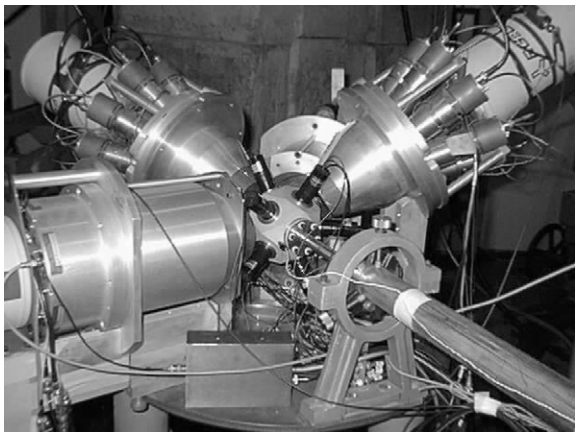

Fig. 3. SACI–PERERE γ-ray spectrometer.

bonding of the interface was usually obtained in 6 h.

A thin layer of aluminium was evaporated over the front face of each detector and the sides were wrapped with teflon tape, in order to prevent cross talk between the detectors and to reflect light from escaping the detector. The complete system SACI and γ-ray spectrometer is shown in Fig. 3.

3. Electronics and data acquisition

A schematic diagram of the electronics used with the detector system is shown in Fig. 4. The signal from the photomultiplier tube consists of two components: a fast one due to the ΔE scintillator and a second one with a much longer decay constant from the E detector [8]. The output signal of the photomultiplier tube goes to the *Linear Fan-In/Fan-Out* in order to produce two signals: one to generate the timing signals (fast gate GR and slow gate GL), and the second signal to be integrated by the charge ADCs during the presence of the respective common gates. In our case the E signal was integrated by the LeCroy 2249 W *Charge ADC with Wide Gates* (QDCW) during 200 ns, starting about 50 ns after the rise of the ΔE signal, which is integrated by the LeCroy 2249 A *Charge ADC* (QDCA) during 30 ns. The gate settings influence the particle separation in the $\Delta E - E$ spectrum. A good selection of the integration time is necessary to minimize the intrinsic pedestal, which is proportional to the width of the gate, and to avoid any reflection of the fast signal [9–12].

A timing signal is produced in the *Timing Filter Discriminator* (TFD) and the output goes to the *Logic Fan-In/Fan-Out* module which receives a signal from any of the other phoswich detectors. The coincidence between the γ-Event (E_γ) and the particles is verified by the *Coincidence Unit* (AND E_γ–p). The Compton suppressed γ–γ coincidence is verified several 100 ns after the charged particle pulse. The QDCs must start the conversion before the coincidence is verified, otherwise the signal of the particle detectors becomes degraded when delayed for such long times, impairing the identification of charged particles (a sufficiently high pass delay line is not yet available). If there is coincidence the conversion is completed, otherwise it is aborted to avoid rate limitations associated with saturation of the data acquisition system, and to avoid increase in the dead time. The Event trigger is produced by the single γ or γ–γ coincidence, depending on the specific experiment.

In typical experiments, the counting rate of the HPGe γ-ray detectors is limited to less than 10 kHz in order to avoid pulse pileup, while the

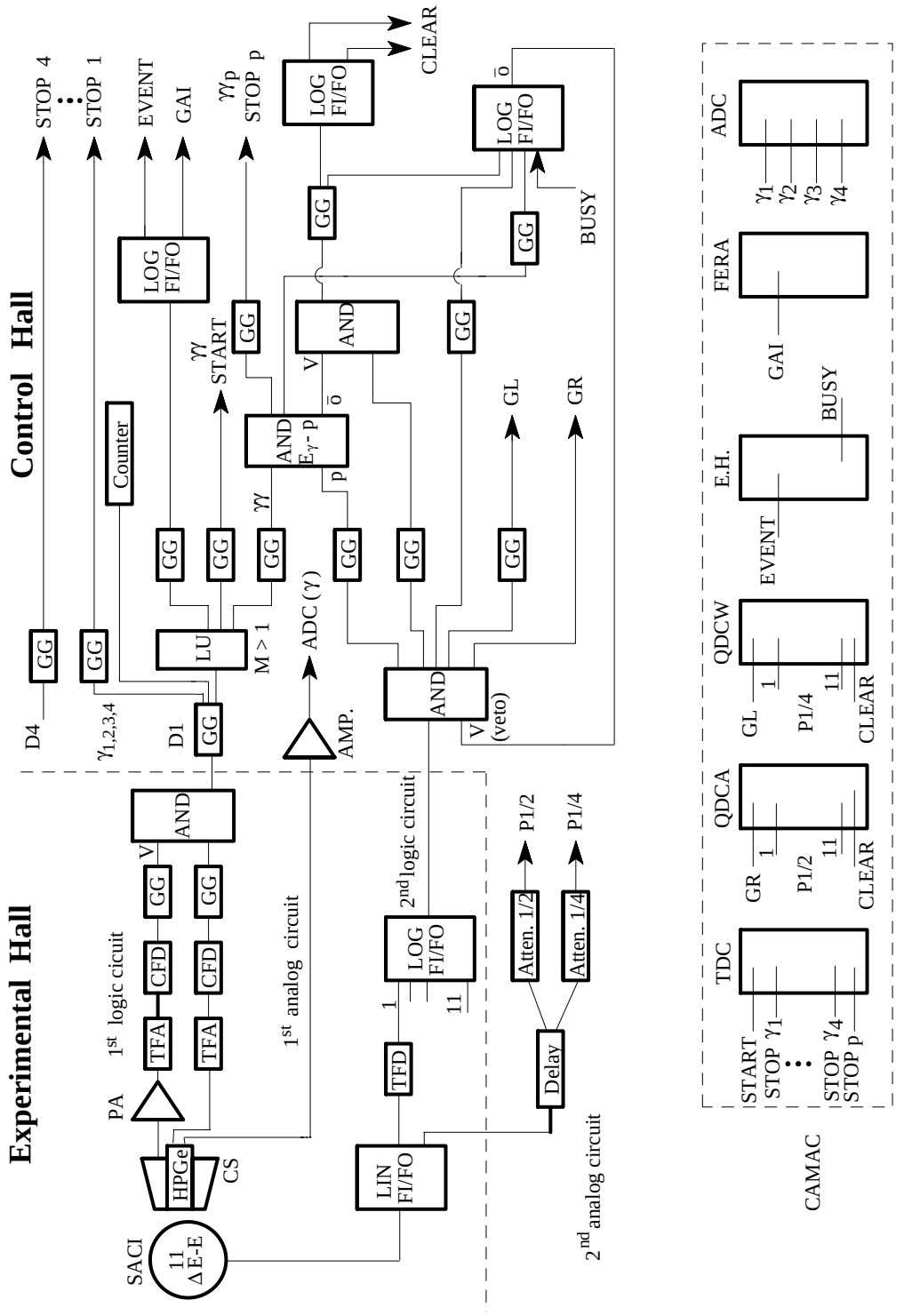

Fig. 4. A schematic diagram of the electronics used.

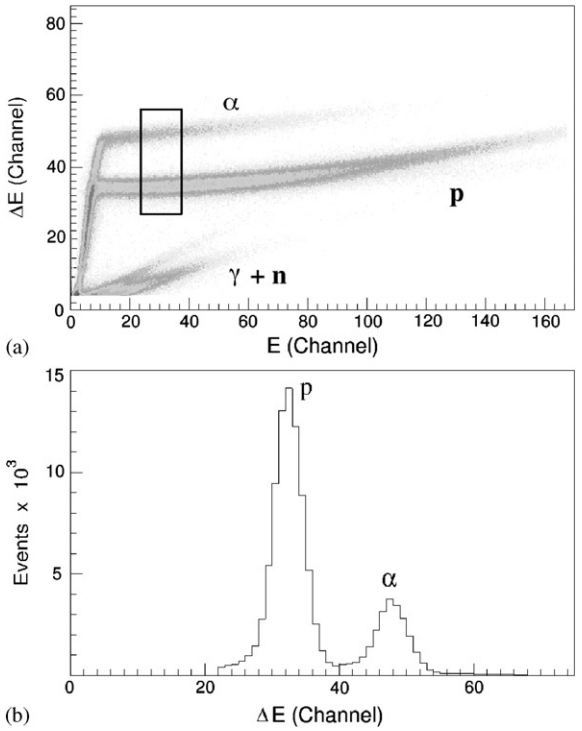

Fig. 5. (a) $\Delta E - E$ particle spectrum taken with 43 MeV ^{11}B ions on a target of ^{100}Mo and (b) Projection on the ΔE axis of the window enclosed by the box in a.

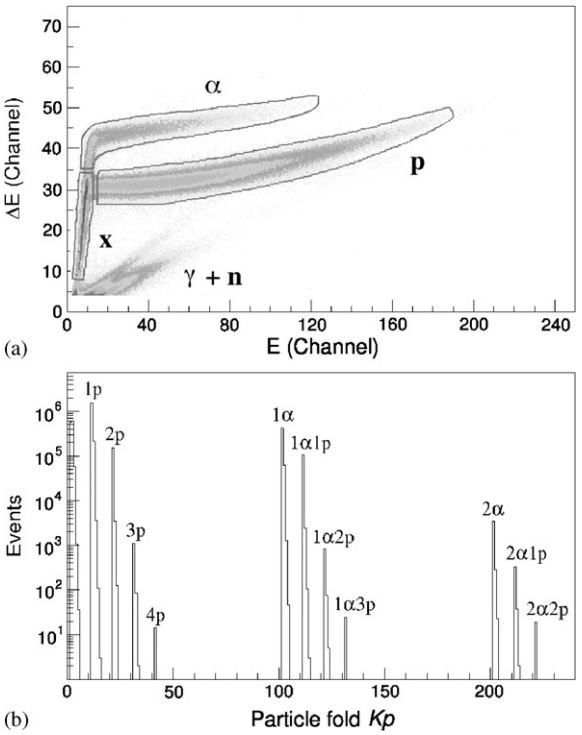

Fig. 6. (a) $\Delta E - E$ particle spectrum taken with 53 MeV ^{16}O ions on a target of ^{27}Al showing the 2D-gates for different particles and (b) Particle fold (K_p) spectrum.

rate of the particle pulses produced in a reaction is approx. 180 kHz. The dead time of the QDC system is ≈ 3 μs, resulting in a dead time fraction of $\sim 20\%$ for the charged particle detectors. The use of two QDCs in parallel is being considered as a possible means of reducing the dead time.

4. In-beam test and performance of the detector system

In-beam tests were performed using the known reactions, ^{27}Al $+^{16}$O at 53 MeV [13], and ^{100}Mo $+^{11}$B at 43 MeV [14]. The beams were provided by the Pelletron tandem accelerator of the University of São Paulo. The targets used were a ≈ 3 mg/cm^2 thick ^{27}Al foil pressed on to Pb backing to stop the recoils, and a ≈ 18 mg/cm^2 thick metallic self-supporting foil of enriched ^{100}Mo, respectively. In the front face of each detector enough aluminium foils were placed to avoid scattered beam. The quantity of aluminium depends on target thickness and the angle of the particle detector, through the energy of the scattered beam. Many residual nuclei were populated via the evaporation of $x\alpha\, yp\, zn$.

Events were collected on tape when at least two HPGe detectors fired in coincidence. The data from phoswich detectors, if present, were acquired together with the γ–γ coincidence parameters. Events were stored in event mode on a magnetic tape and the analysis was made off-line, using the VPAK [15] data analysis package.

The $\Delta E - E$ matrix obtained from 43 MeV ^{11}B ions on a target of ^{100}Mo is presented in Fig. 5a. This figure shows the quality of particle identification. Particles with $Z = 1$ and 2 (mainly protons and α particles) as well as pulses from γ-rays and/or neutrons are shown. Different isotopes (p, d, and t or α particles and ^{3}He) if present, cannot be

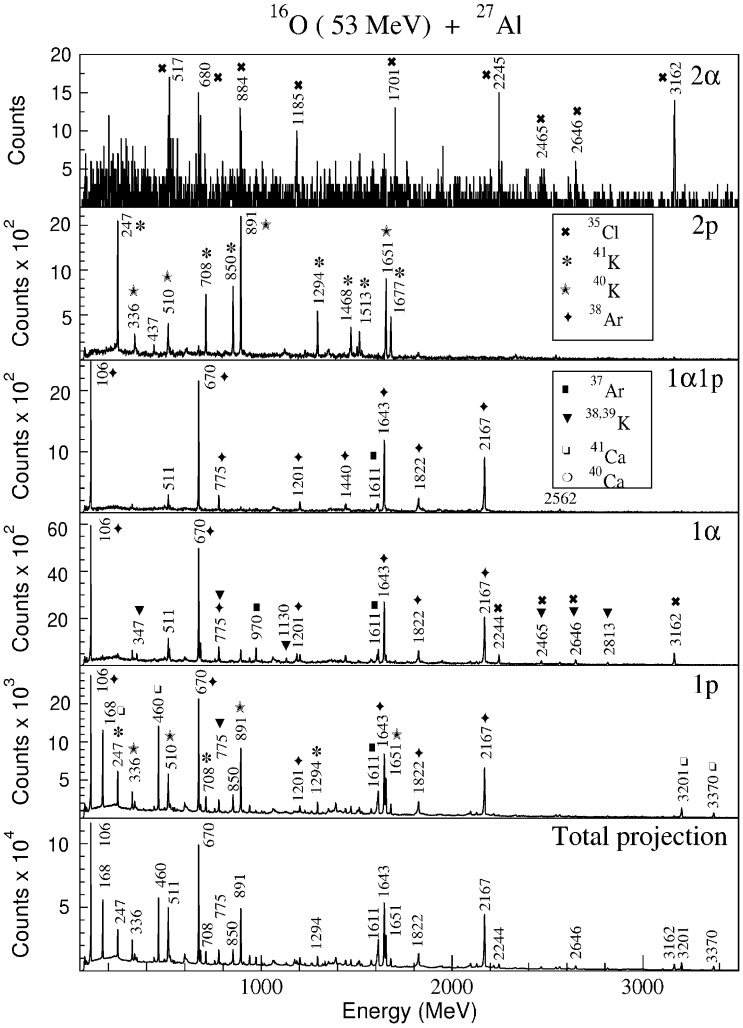

Fig. 7. γ-ray spectra with different particle fold gates (K_p) taken with 53 MeV ^{16}O ions on a target of ^{27}Al. This figure shows from top to bottom 2α, 2p, 1α1p, 1α, 1p gates and total projection.

separated. Fig. 5b, shows a projection on the ΔE axis of the window enclosed by the box in Fig. 5a. A clear separation between proton and α particle events was obtained.

A new parameter called particle fold (K_p) was created off-line using different 2D-gates for different particles. Fig. 6a shows the α particle and proton gate. A third gate (x) corresponds to the charged particles which stopped in ΔE detectors which cannot be identified. To determine K_p the following relationship was used:

$$K_p = 100(n_\alpha) + 10(n_p) + 1(n_x)$$

where n_α and n_p are the number of α particles and protons, respectively; n_x represents the number of charged particles (p and α) which stop in the ΔE detector. In this way, the particle types and respective folds are determined. It is important to remark that events from 1α1p, 2p channels and 1α1p, 2α channels, for example, will appear in 1p

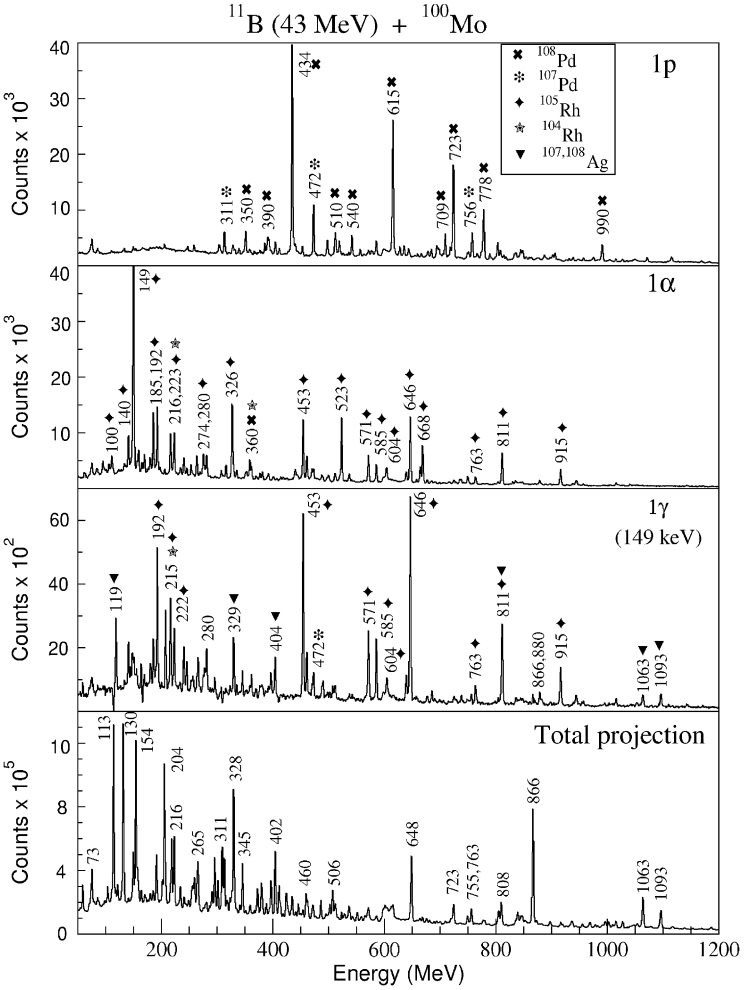

Fig. 8. γ-ray spectra with different particle fold gates (K_p) taken with 43 MeV ^{11}B ions on a target of ^{100}Mo. This figure shows from top to bottom 1p, 1α, 1γ gates and total projection.

and 1α spectra, respectively, due to the escape from detection in the charged particle array of one proton or α particle. Channels containing any number of neutrons will also appear in the spectra because the neutrons were not detected. A linear combination of particle gated γ–γ matrices can be used, if necessary, to generate clean spectra consisting of transitions from each individual charged particle multiplicity channel of the reaction. The effectiveness of SACI in the selection of the reaction channel is illustrated in Figs. 7 and 8, which show examples of γ spectra requiring the coincidence with various combinations of light charged particles as detected in the ancillary system.

In Fig. 8, the panel labeled 1γ (149 keV) shows the projection of γ–γ matrix in coincidence with the 149 keV transition from ^{105}Rh. γ-rays of about 149 keV exist also in ^{107,108}Ag and as a result one can also see several transitions belonging to these nuclei in this spectrum. Requiring, in addition, coincidence with 1α particle, the transitions of ^{107,108}Ag disappear. Therefore, a good separation between γ-rays of different charged particle channels was obtained for both reactions when SACI is used.

Table 1
The experimental particle detection efficiencies from $^{16}O(^{27}Al, x\alpha\, yp\, zn)$ reaction

Channel	Efficiency ε_p (%)	Efficiency ε_α (%)
1α1p (^{38}Ar)	29.3 (16)	12.4 (6)
1α1p1n (^{37}Ar)	13.0 (25)	4.5 (20)
2p (^{41}K)	40.0 (15)	—
2p1n (^{40}K)	27.6 (16)	—
2α (^{35}Cl)	—	4.3 (15)
1p1n (^{41}Ca)	21.5 (6)	—
1p2n (^{40}Ca)	14.3 (7)	—
1α (^{39}K)	—	8.5 (6)
1α1n (^{38}K)	—	5.0 (5)

The particle detection efficiency of SACI is lower than 76% (the geometrical efficiency). It depends on the kinematics of the reactions measured and the thickness of the aluminium absorbers on the front face of each detector, as these foils also absorb part of the low energy evaporated particle spectra. The efficiencies for particle detection from different channels were obtained using *γ–γ-particle* coincidence measurements. The probability $P(D, T)$ to detect D identical particles out of the total T emitted is

$$P(D,T) = \binom{T}{D} \varepsilon^D (1-\varepsilon)^{T-D}$$

where ε is the efficiency for the type of particles. For a charged particle emission channel with two kinds of particles (p and α), we have

$$N_{D_\alpha, D_p} = N^{Tot} \varepsilon_\gamma^1 \varepsilon_\gamma^2 P(D_\alpha, T_\alpha) P(D_p, T_p)$$

where N_{D_α, D_p} is the number of counts in the γ_2 peak in the spectrum gated by γ_1 and D_α, D_p particle gates from T_α, T_p channel. N^{Tot} is the total number reaction events producing the $\gamma_1\gamma_2$ cascade and ε_γ^i are γ-ray detection efficiencies. Using these relationships the particle detection efficiencies were obtained. Thus, from the first reaction, $^{16}O(^{27}Al, x\alpha\, yp\, zn)$, considering the γ-rays from different channels in the spectra with different particle folds, the experimental particle detection efficiencies were determined and the results are shown in Table 1. These values were estimated using 9, 6 and 6 mg/cm^2 of aluminium foils in the front face of each detector at 0°, 37° and 101°, respectively.

From the second reaction $^{11}B(^{100}Mo, x\alpha\, yp\, zn)$, the values of the efficiencies obtained for protons in the 1p2n channel (^{108}Pd) and alphas in the 1α2n channel (^{105}Rh) were, respectively, 25.3 (6)% and 3.5 (5)%. For the 1p3n (^{107}Pd) and 1α3n (^{104}Rh) channels the small cross-sections did not allow the determination of the particle efficiencies.

The particle detection efficiencies are different for different particle channels and decrease when more particles are emitted from a respective channel. This can be understood by considering that the average energy of the particles tends to be lower when more particles are evaporated. In summary, the particle detection efficiency depends on the type and kinematics of the reaction used, and the particle detection threshold.

We define the *resolving power* as the improvement factor (F) of the peak-to-background (P/B) ratio, when a specific particle fold is required. The experimental values of F for some transitions in ^{40,41}K (2p particle fold) produced in the first reaction are shown in Table 2. Fig. 9 shows the

Table 2
The experimental improvement factor F for some transitions from ^{40,41}K (2p particle fold) produced using ^{16}O ($^{27}Al, x\alpha\, yp\, zn$) reaction

Energy (keV)	K_p	P/B	F
1227[a]	2p	0.71 (16)	4.99 (14)
	1p	0.16 (1)	1.09 (7)
	Total proj.	0.14 (1)	
1293[a]	2p	3.71 (66)	5.82 (5)
	1p	0.77 (2)	1.21 (3)
	Total proj.	0.64 (1)	
1468[a]	2p	2.50 (47)	4.88 (6)
	1p	0.61 (2)	1.19 (4)
	Total proj.	0.51 (1)	
1500[a]	2p	1.07 (25)	3.93 (9)
	1p	0.31 (2)	1.16 (6)
	Total proj.	0.27 (1)	
1512[a]	2p	3.05 (65)	5.45 (5)
	1p	0.68 (2)	1.21 (3)
	Total proj.	0.56 (1)	
1526[b]	2p	1.39 (33)	5.68 (10)
	1p	0.25 (1)	1.03 (6)
	Total proj.	0.24 (1)	

[a] γ-ray from ^{41}K.
[b] γ-ray from ^{40}K.

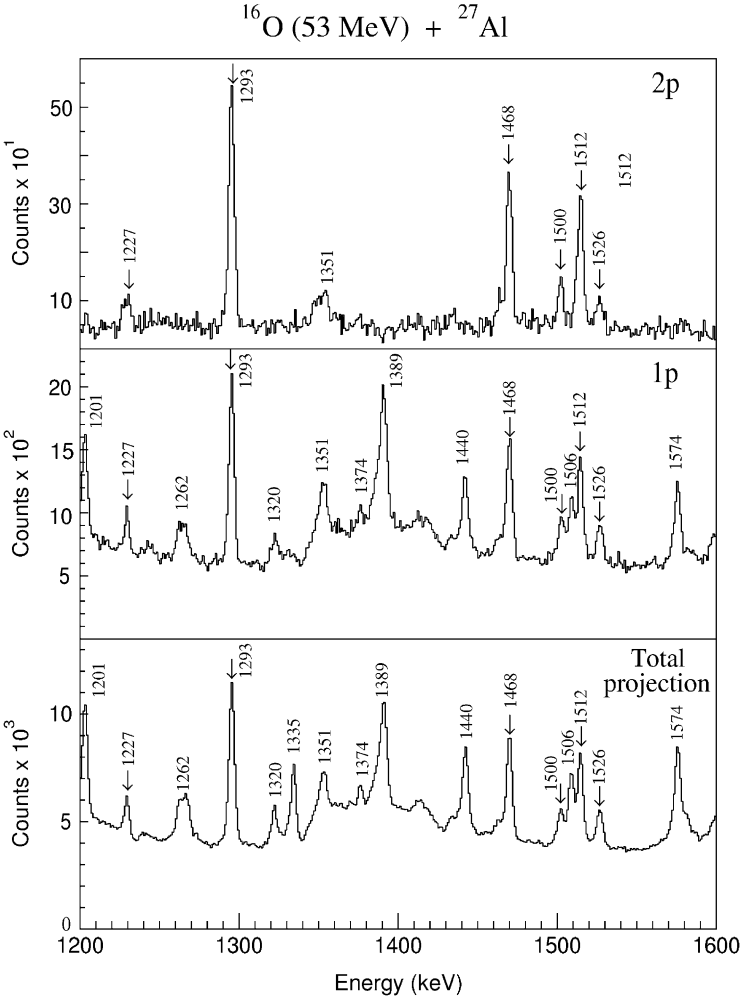

Fig. 9. γ-ray spectra with $K_p = 1p, 2p$ and total projection, taken with 53 MeV ^{16}O ions on a target of ^{27}Al. This figure shows from top to bottom 2p, 1p gates and total projection. See improvement of P/B ratio for some transitions from $^{40,41}K$ (marked with arrow), when SACI is used.

increase of the P/B ratio for several γ transitions from $^{40,41}K$.

On average, there is an improvement in the peak to background ratio of $\langle F \rangle \simeq 5.1$ for the 2p particle fold compared to the 1p particle fold. The reason for this improvement is that at the incident energy used, those 3p particle channels which contribute to the 2p fold spectra are much less in number than the sum of 2p and 3p particle channels which contribute to the background in the 1p fold gate.

In the second reaction, the 1α channel selection permitted improved observation of the ^{105}Rh nucleus and many new bands were identified in this nucleus [16]. At 43 MeV beam energy the ^{105}Rh nucleus has a factor of 9 and 3 less cross-section than $^{107,108}Ag$, respectively. In Fig. 10, one can see clearly the improvement in the P/B ratio for several ^{105}Rh transitions, $\langle F \rangle \simeq 10.0$, when gates are placed on the 1α channel together with the 149 keV γ from ^{105}Rh. The 119 and 164 keV γ-rays appearing in the 1γ-gate spectrum

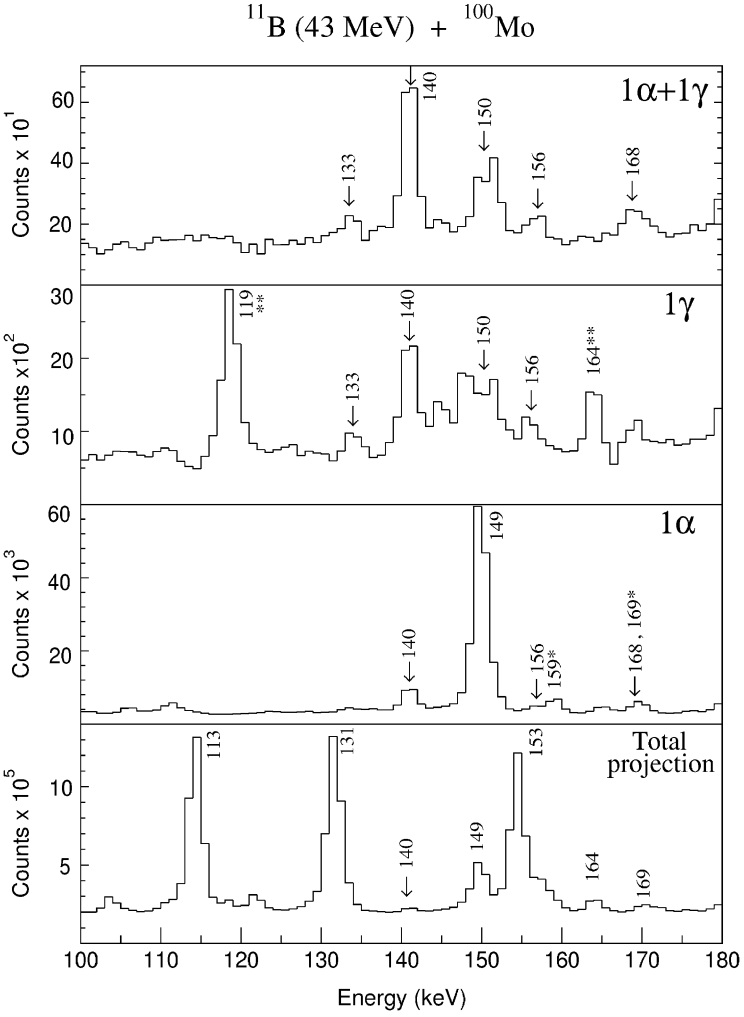

Fig. 10. γ-ray spectra with $K_p = 1\alpha$ and total projection taken with 43 MeV ^{11}B ions on a target of ^{100}Mo. This figure shows from top to bottom 1α1γ (149 keV), 1γ (149 keV), 1α gates and total projection. See enhancement of P/B ratio for 133, 140, 150, 156 and 168 keV from ^{105}Rh, when SACI is used. (*) Transitions belonging to ^{104}Rh. (**) Contaminants.

in Fig. 10 are from a contaminant reaction channel.

5. Conclusion

This paper reports the construction and tests of SACI, a large solid-angle phoswich scintillator system for detection of light charged particles, to be used as an ancillary component of the γ-ray spectrometer at the Pelletron Laboratory of the University of São Paulo. The SACI showed good results for the identification and separation between α particles and protons. The particle detection efficiency and the resolving power obtained are dependent on the specific reaction. The channel selection permits an easier identification of the charged particle component of the evaporation, and results in a substantial improvement in peak-to-background ratio for weak evaporation channels. This improvement permitted the observation of new transitions

previously unidentified in ^{105}Rh [16]. The improvement factor F and particle detection efficiency obtained are considered acceptable for the usefulness of the system.

Acknowledgements

We thank the staff of the tandem Pelletron accelerator of the University of São Paulo. This work was partially supported by the Fundação de Amparo à Pesquisa do Estado de São Paulo (FAPESP) and the Conselho Nacional de Desenvolvimento Científico e Tecnológico (CNPq), Brazil.

References

[1] E. Farnea, et al., Nucl. Instr. and Meth. A 400 (1997) 87.
[2] D.G. Sarantites, et al., Nucl. Instr. and Meth. A 381 (1996) 418.
[3] R. Ribas, et al., Annual Report of the Nuclear Physics Department, Institute of Physics, University of São Paulo, 1996, p. 63.
[4] F. Lidén, Nucl. Instr. and Meth. A 288 (1990) 455.
[5] Technical Manual, Bicron Corporation, Newbury, OH, USA, 1990.
[6] C.A. Pruneau, et al., Nucl. Instr. and Meth. A 297 (1990) 404.
[7] J. Alcántara-Núñez, et al., Annual Report of the Nuclear Physics Department, Institute of Physics, University of São Paulo, 1998, p. 52.
[8] D.H. Wilkinson, Rev. Sci. Instrum. 23 (1952) 414.
[9] F. Lidén, et al., Nucl. Instr. and Meth. A 253 (1987) 305.
[10] F. Lidén, et al., Nucl. Instr. and Meth. A 273 (1988) 240.
[11] C. Pastor, et al., Nucl. Instr. and Meth. A 212 (1983) 209.
[12] T. Chapuran, et al., Nucl. Instr. and Meth. A 272 (1988) 767.
[13] J. Dauk, et al., Nucl. Phys. A 241 (1975) 170.
[14] F. Espinoza-Quiñones, et al., Phys. Rev. C 55 (1997) 2787.
[15] W.T. Milner, Holifield Heavy Ion Research Facility Computer Handbook, Oak Ridge National Laboratory, Oak Ridge, TN, USA, 1987.
[16] E. Cybulska, et al., Acta Phys. Pol. B 32 (2001) 929.